

Chasing Long-Lived Doubly Charged Scalars at Future Lepton Colliders

Nandini Das,^{a,b} Dilip Kumar Ghosh,^c Nivedita Ghosh,^d Ritesh K. Singh^e

^a*Department of Physics, SGTB Khalsa College, Delhi 110007, India*

^b*Department of Physics and Astrophysics, University of Delhi, Delhi 110007, India*

^c*School of Physical Sciences, Indian Association for the Cultivation of Science, 2A & 2B, Raja S.C. Mullick Road, Kolkata 700032, India*

^d*Kavli IPMU (WPI), UTIAS, University of Tokyo, Kashiwa, Chiba, 277-8583, Japan*

^e*Department of Physical Sciences, Indian Institute of Science Education and Research Kolkata, Mohanpur, 741246, Nadia, India*

E-mail: nandinidas.rs@gmail.com, tpdkg@iacs.res.in,
nivedita.ghosh@ipmu.jp, ritesh.singh@iiserkol.ac.in

ABSTRACT: We come up with a novel search strategy for long-lived doubly charged scalars at future proposed lepton colliders. The doubly charged scalar studied in this work belongs to an $SU(2)_L$ complex scalar triplet that accounts for tiny neutrino masses via the Type-II Seesaw mechanism. For scalar masses $\lesssim 200$ GeV and appropriate values of the triplet vacuum expectation value, this state can be long-lived and decay predominantly into like-sign muon pairs (e.g. $\mu^+\mu^+$ or $\mu^-\mu^-$), producing distinctive displaced-vertex signals. We investigate the pair production of these scalars at the International Linear Collider (ILC) and a prospective muon collider, considering their planned center-of-mass energies. Incorporating theoretical and experimental constraints, we study the resulting signature of four leptons accompanied by missing transverse energy. Displaced vertices offer direct evidence of the scalar's long lifetime, while we further show that the invariant mass distribution of same-sign dilepton pairs serves as a powerful complementary probe for discovering doubly charged Higgs bosons at both the ILC and muon collider.

Contents

1	Introduction	1
2	Model	3
3	Theoretical and Experimental Constraints	5
4	Collider Analysis	7
4.1	Pair production of the doubly-charged Higgs via Drell-Yan process at the ILC	8
4.2	Pair production of doubly charged Higgs at muon collider with missing energy	11
5	Conclusion	17

1 Introduction

A decade after the Higgs discovery [1, 2], the non-observation of any Beyond the Standard Model (BSM) signals at the collider urges us to revisit the underlying search techniques. Most of the searches at the colliders assume that the new physics (NP) particles decay promptly. But this need not be true, as even within the SM, we have mesons and baryons which are Long-Lived Particles (LLPs) [3], i.e., they have a proper decay length $c\tau \gtrsim \mathcal{O}(\text{mm})$ in the detector. The possibility that NP particles can be long-lived has important consequences in the collider searches [4, 5]. In particular, searches for scalar LLPs have long been one of the central focus of beam-dump experiments such as SHiP [6], NA62 [7], and NA64 [8], as well as collider-based experiments at the Large Hadron Collider (LHC) [9–18], the International Linear Collider (ILC) [19], and proposed future circular colliders (FCC) [20–24]. The phenomenology of scalar LLPs has also been extensively explored at low-energy e^+e^- colliders, such as Belle II [25], as well as at neutrino facilities [26, 27].

In a different context, the generation of tiny nonzero neutrino masses through the seesaw mechanism can be realized in the Type-II seesaw model [28–32]. The scenario extends the SM by introducing a $SU(2)_L$ complex triplet scalar, where lepton number

is violated by two units through a trilinear coupling μ in the scalar potential. Neutrinos acquire Majorana masses via the Yukawa interaction between the triplet and the lepton doublets, leading to $m_\nu \sim \frac{Y_\Delta \mu v_d^2}{M_\Delta^2}$, with M_Δ being the triplet mass and v_d being the vacuum expectation value of the SM Higgs doublet (**vev**). The smallness of m_ν can thus be explained by a naturally small μ term, protected by symmetry in the sense of '*t Hooft* naturalness [33]. The same μ term generates the triplet vev $v_t \sim \frac{\mu v_d^2}{M_\Delta^2}$, which is induced after the electroweak symmetry breaking. An appropriate choice of (μ or v_t) and Y_Δ , consistent with current neutrino oscillation data [34], allows one to obtain tiny neutrino masses even for triplet scalars near the electroweak scale ($M_\Delta \sim v_d$). Additionally, the presence of the exotic singly and doubly charged scalars makes this model phenomenologically appealing for collider studies. In particular, the most striking signature of the triplet extension is the appearance of a doubly charged scalar, which offers distinctive and experimentally accessible collider signals.

Depending on the triplet vev, the doubly charged scalar can decay to a pair of dileptons of the same-sign ($v_t < 10^{-4}$ GeV), or a pair of gauge bosons ($v_t > 10^{-4}$ GeV) [35–37]. The ATLAS [14, 38–41] and CMS [42–44] collaborations have searched for these doubly charged scalars $H^{\pm\pm}$ in both pure leptonic and $W^\pm W^\pm$ final states at $\sqrt{s} = 13$ TeV, assuming prompt decay of the scalar. The non-observance of any significant excess at the LHC has put an upper limit on the mass of the doubly charged scalar to be > 1080 GeV for $v_t < 10^{-4}$ GeV [40]. However, one should keep in mind that all these null results are derived assuming that the doubly-charged scalar decays promptly. The possibility that these scalar particles may not decay promptly, but instead exhibit long-lived behavior, carries important implications for their search strategies at the collider. Searches for such heavy stable charged particles (HSCPs) have already been performed by ATLAS [45, 46] and CMS [47, 48]. If the decays of a long-lived particle are non-prompt but occur inside the detector volume, displaced secondary vertices can also serve as a powerful probe. This possibility has recently been explored in recent literature in the context of the Type-II seesaw model [49, 50]. However, the search for displaced vertex search for the doubly-charged scalars at the lepton colliders is scarce in the literature.

In this paper, we rekindle the idea of probing the doubly-charged scalar as a long-lived particle in future precision collider facilities such as the International Linear Collider (ILC) [51–56] and the International Muon Collider Collaboration (IMCC) [57–63]. Compared to the hadron colliders, because of the added advantage of being less noisy, the lepton colliders may act as a discovery machine for the doubly charged Higgs boson.

To be more specific, we produce the doubly charged scalar in pairs in the proposed 500 GeV ILC machine with 4 ab^{-1} integrated luminosity [64] whereas we pair produce the doubly charged scalars with a pair of fermions in the proposed 10 TeV muon collider with 10 ab^{-1} luminosity [65, 66]. We find out that owing to the cleaner environment of the colliders, with a few to a few hundred fb^{-1} of luminosity, we can discover the doubly charged scalar in the mass range $\in [100 : 180] \text{ GeV}$ by looking at the long-lived di-muonic decays of the scalar.

The paper is organized as follows. In Section 2, we briefly discuss the model, followed by theoretical and experimental constraints on our model parameter space in Section 3. We motivate our analysis strategy and results in Section 4. Finally, we conclude in Section 5.

2 Model

In this section, we briefly outline the Type-II seesaw model, which augments the Standard Model (SM) with a $SU(2)_L$ complex triplet scalar field Δ of hypercharge $Y = 2$ given by

$$\Delta = \frac{\sigma^i}{\sqrt{2}} \Delta_i = \begin{pmatrix} \delta^+/\sqrt{2} & \delta^{++} \\ \delta^0 & -\delta^+/\sqrt{2} \end{pmatrix}, \quad (2.1)$$

Here σ_i 's correspond to the Pauli matrices where i runs from one to three and $\Delta_1 = (\delta^{++} + \delta^0)/\sqrt{2}$, $\Delta_2 = i(\delta^{++} - \delta^0)/\sqrt{2}$, $\Delta_3 = \delta^+$. The Lagrangian of the model, incorporating the SM with the triplet sector, is given by

$$\mathcal{L} = \mathcal{L}_{\text{Yukawa}}^{\Delta+\text{SM}} + \mathcal{L}_{\text{Scalar}}^{\Delta+H} + \mathcal{L}_{\text{Gauge}}^{\text{SM}} \quad (2.2)$$

where the scalar part is composed of

$$\mathcal{L}_{\text{Scalar}}^{\Delta+H} = \mathcal{L}_{\text{Kinetic}} - V(\Phi, \Delta), \quad (2.3)$$

The kinetic and Yukawa interactions are, respectively, [67]

$$\mathcal{L}_{\text{Kinetic}} = (D_\mu \Phi)^\dagger (D^\mu \Phi) + \text{Tr} \left[(D_\mu \Delta)^\dagger (D^\mu \Delta) \right], \quad (2.4)$$

$$\mathcal{L}_{\Delta+\text{SM}}^{\text{Yukawa}} = \mathcal{L}_{\text{Yukawa}}^{\text{SM}} - (Y_\Delta)_{ij} L_i^\text{T} C i\sigma_2 \Delta L_j + \text{h.c.} \quad (2.5)$$

Here, $\Phi^\text{T} = (\phi^+ \ \phi^0)$ is the SM scalar doublet, L represents the $SU(2)_L$ left-handed

lepton doublet, Y_Δ is the Yukawa coupling, and C is the Dirac charge conjugation matrix. The covariant derivative of the scalar triplet field is given by:

$$D_\mu \Delta = \partial_\mu \Delta + i \frac{g}{2} [\sigma^a W_\mu^a, \Delta] + ig' B_\mu \Delta \quad (a = 1, 2, 3). \quad (2.6)$$

σ^a are the Pauli matrices, g and g' are the gauge coupling constants of the $SU(2)_L$ and $U(1)_Y$ group, respectively.

The most general scalar potential can be written as [67]:

$$\begin{aligned} V(\Phi, \Delta) = & -m_\Phi^2 (\Phi^\dagger \Phi) + \frac{\lambda}{4} (\Phi^\dagger \Phi)^2 + M_\Delta^2 \text{Tr}(\Delta^\dagger \Delta) + (\mu \Phi^\top i \sigma_2 \Delta^\dagger \Phi + \text{h.c.}) + \\ & \lambda_1 (\Phi^\dagger \Phi) \text{Tr}(\Delta^\dagger \Delta) + \lambda_2 [\text{Tr}(\Delta^\dagger \Delta)]^2 + \lambda_3 \text{Tr}(\Delta^\dagger \Delta)^2 + \\ & \lambda_4 \Phi^\dagger \Delta \Delta^\dagger \Phi. \end{aligned} \quad (2.7)$$

In general, all the parameters of the potential can be complex. However, for simplicity, we have assumed that they are real.

After EWSB, the neutral component of the scalar fields expanded around the respective vevs can be parametrized as

$$\Phi = \frac{1}{\sqrt{2}} \begin{pmatrix} \sqrt{2} \chi_d^+ \\ v_d + h_d + i \eta_d \end{pmatrix} \quad \Delta = \frac{1}{\sqrt{2}} \begin{pmatrix} \delta^+ & \sqrt{2} \delta^{++} \\ v_t + h_t + i \eta_t & -\delta^+ \end{pmatrix}. \quad (2.8)$$

where v_d and v_t denote the doublet and triplet vacuum expectation values (VEV), respectively. Similarly, minimizing the potential, the two mass parameters of the potential can be written in terms of the other free parameters as

$$m_\Phi^2 = \lambda \frac{v_d^2}{4} - \sqrt{2} \mu v_t + \frac{(\lambda_1 + \lambda_4)}{2} v_t^2, \quad (2.9)$$

$$M_\Delta^2 = \frac{\mu v_d^2}{\sqrt{2} v_t} - \frac{\lambda_1 + \lambda_4}{2} v_d^2 - (\lambda_2 + \lambda_3) v_t^2, \quad (2.10)$$

The scalar spectrum of the model is brought down to the mass basis from the gauge basis by orthogonal rotation in the CP-even, CP-odd, and charged sector with rotation angles α, β and β' respectively giving us seven physical Higgs bosons, namely two doubly charged $H^{\pm\pm}$, two singly charged H^\pm , two CP-even neutral (h, H) and a CP-odd (A) scalar. For more details, see [68]. Although no extension of the SM gauge sector is needed for the inclusion of this triplet scalar, the electroweak gauge boson masses (M_W, M_Z) get a finite contribution from the triplet VEV (v_t) at tree level, which in turn modifies the ρ parameter. Precision electroweak data constrain

the ρ parameter to be very close to its SM value of unity [3], which imposes an upper bound on v_t of $v_t \lesssim 2.1$ GeV [50]. On the other hand, the non-standard triplet Yukawa Lagrangian gives rise to the neutrino mass where the mass matrix is given by $M_\nu = \sqrt{2}v_t Y_\Delta$. This mass matrix is diagonalized by the neutrino mixing matrix, i.e., the Pontecorvo–Maki–Nakagawa–Sakata (PMNS) matrix, whose elements are determined from neutrino oscillation data for a given neutrino mass hierarchy [69, 70]. Consequently, a neutrino mass of $\mathcal{O}(0.1)$ eV can be realized by appropriately tuning either the triplet VEV (v_t) or the Yukawa coupling (Y_Δ). For $v_t \sim \mathcal{O}(1)$ GeV, the Yukawa coupling must be small, whereas an order-one neutrino Yukawa coupling ($Y_\Delta \sim \mathcal{O}(1)$) requires $v_t < \mathcal{O}(10^{-4})$ eV. These two cases represent the extreme limits of the triplet VEV.

3 Theoretical and Experimental Constraints

In this section, we provide a brief overview of the existing theoretical and experimental constraints applicable to our benchmark choices:

- **Vacuum stability:** To have the scalar potential bounded from below in all directions in field space, we have taken into account all the necessary and sufficient conditions on the scalar quartic couplings mentioned in [67].
- **Perturbative unitarity:** The requirement of perturbativity of the quartic couplings as well as the tree-level unitarity of the scattering amplitude for all $2 \rightarrow 2$ processes requires the \mathcal{S} -matrix eigenvalues to be bounded from above ($|a_i| < 16\pi$). The set of unitarity conditions received from the above requirements for this scalar setup [67] is satisfied by the benchmark points considered in our analysis.
- **Constraints from electroweak precision test:** The presence of the new exotic scalar bosons contributes to the electroweak precision observables, parametrized by the oblique coefficients S, T, and U [71, 72]. Among these, the strongest bound comes from the T-parameter, which imposes a strict limit on the mass splitting between the doubly and singly charged scalars, $\Delta M \equiv |m_{H^{\pm\pm}} - m_{H^\pm}| \equiv |m_{H^\pm} - m_H/m_A|$ which should be $\lesssim 50$ GeV [73]. Our scalar spectrum corresponding to the multiplet, being almost degenerate, is safe from this constraint.
- **Higgs Signal Strength:** The observed SM-like Higgs boson with a mass of 125 GeV, and therefore its decay widths, must remain consistent with the Higgs measurements reported at the LHC. The benchmark points are chosen such that the

diphoton signal strength remains within the 2σ limit of the current experimental bound of the Higgs to diphoton signal strength 1.13 ± 0.09 [74].

- **Experimental bounds on the scalar masses:** The direct search for the non-standard scalars has a strong impact on our model parameter space. The direct search on the singly charged scalar in LEP II places a limit on $m_{H^\pm} \geq 80$ GeV [75]. LHC has also searched for the decay of $t \rightarrow H^+ b$ [76] and $H^+ \rightarrow t\bar{b}$ [77] depending on the mass H^\pm . However, for the type-II seesaw model, this coupling is v_t/v_d suppressed, which does not affect our parameter space.

Collider searches for the non-standard neutral Higgs have also been done in detail at the LHC [78, 79]. However, for this model, production of the nonstandard scalars is suppressed by $(v_t/v_d)^2$ and hence does not affect our parameter region.

The search for doubly charged Higgs in the multi-lepton final state is done in ATLAS [40] assuming that the doubly charged Higgs decays promptly and masses $\in [300:1080]$ GeV have been excluded. There is also a bound on doubly-charged Higgs from the production of same-sign W-boson pairs $\in [200:220]$ GeV [38]. CMS has also searched for the doubly-charged scalar at 13 TeV [47, 48]. However, all searches assume that the scalar decays promptly.

- **Long-lived $H^{\pm\pm}$:** The scenario changes significantly if the doubly charged scalar is **long-lived**. Depending on the triplet vev and the mass of the doubly charged Higgs, it can decay into a pair of same-sign dileptons, a pair of same-sign gauge bosons, or undergo a three-body decay via $H^{\pm\pm} \rightarrow W^\pm (W^\pm)^* \rightarrow W^\pm f\bar{f}$, as discussed in Ref. [80]. By appropriately tuning the triplet vacuum expectation value v_t and $m_{H^{\pm\pm}}$, the total decay width $\Gamma_{H^{\pm\pm}}$ of the doubly charged Higgs can be made very small $\Gamma_{H^{\pm\pm}} \lesssim 10^{-14}$ GeV. Such an extremely narrow width corresponds to a macroscopic proper decay length $c\tau \gtrsim \mathcal{O}(0.1 \text{ mm})$, rendering a long-lived particle(LLP) in collider detectors. A comprehensive analysis of this scenario has been performed in [50]. After imposing all the present constraints, a region of model parameter space remains viable with

$$m_{H^{\pm\pm}} \in [89, 200] \text{ GeV}, \quad v_t \in [10^{-4}, 10^{-3}] \text{ GeV}, \quad (3.1)$$

where the doubly charged Higgs can evade existing bounds while showing a displaced or long-lived decay signature.

Taking into account all the constraints discussed so far, we choose our benchmark points as mentioned in Table 1. To satisfy all the constraints, we need the non-standard

scalar masses to be degenerate. For our choice of v_T , the doublet-triplet CP even scalar mixing angle α is $< 10^{-5}$. The value of the parameters for each benchmark and the corresponding proper decay lengths $c\tau$ of the doubly charged scalar and its branching ratios into muons are shown. As the mass of the doubly-charged scalar increases, the decay width increases, leading to a drop in $c\tau$. Once the $W^\pm W^\pm$ decay channel becomes kinematically accessible (third benchmark), the decay width increases drastically, resulting in a highly suppressed $c\tau$. And the corresponding branching ratio of $H^{\pm\pm}$ in the dimuon channel also drops.

	$H^{\pm\pm}$ (GeV)	v_t (GeV)	$c\tau$ (mm)	Branching Ratio to muons
BP1	100	9.0×10^{-4}	26.2	19.5%
BP2	120	5.0×10^{-4}	8.6	17.2%
BP3	180	1.6×10^{-4}	0.14	6.1%

Table 1. Benchmark points satisfied by all the theoretical and experimental constraints.

4 Collider Analysis

Our main goal is to explore the long-lived nature of the doubly charged scalars through their leptonic decay at future leptonic colliders. For this purpose, we focus on the model parameter space that provides $M_{H^{\pm\pm}} \sim 100 - 200$ GeV with some fine-tuned choices of v_t . The choice of model parameters is such that $H^{\pm\pm}$ predominantly decays to $\mu^\pm \mu^\pm$ final state. At the lepton colliders, such a doubly charged scalar can be pair-produced either via the canonical Drell-Yan process or via the vector boson fusion (VBF) mode. The mass of the final particles being in the range of [100 – 200] GeV, the Drell-Yan cross-section is considerable to probe at a lepton collider with $\sqrt{s} \sim [200 - 400]$ GeV, while the vector boson fusion cross-section is order of magnitude smaller compared to it. Therefore, ILC planned to operate in the ballpark of this energy, which can offer a good environment for probing the Drell-Yan production. But with increasing CM energy, $\sqrt{s} \sim \mathcal{O}(1)$ TeV, the Drell-Yan becomes smaller due to s-channel suppression, while the vector boson fusion can dominate over the Drell-Yan production cross-section. The proposed muon collider with 10 TeV CM energy seems to offer the perfect choice to search for the latter channel. In the latter case, doubly charged scalars are associated with either two forward-moving $\mu^+ \mu^-$ or $\nu_\mu \bar{\nu}_\mu$, depending on the characteristic of the vector boson involved in the fusion process. However, due to the complex structure of the underlying framework and the large particle spectrum, one has to consider other sub-processes involving additional scalars of the model in association with the vanilla VBF contributions for the second production mode. In both cases, our final targets will

be four charged muons emanating from the decays of two doubly charged scalars. In our analysis, we focus on the Drell-Yan process in the ILC environment and the associated production of $H^{\pm\pm}H^{\mp\mp}$ with forward leptons (μ^\pm , or $\nu_\mu\bar{\nu}_\mu$) at a muon collider.

The Drell-Yan signal cross-section at ILC and the VBF cross-section at the muon collider, considering the muonic decay of the doubly charged Higgs, for three benchmark points are mentioned in Table 2 for two sets of CM energy, $\sqrt{s} = 500$ GeV and $\sqrt{s} = 10$ TeV. As discussed before, for low energy, Drell-Yan performs better, whereas for higher energy, VBF is a better bet. The type II seesaw model specific details enter the analysis via the branching ratio of the doubly charged Higgs to the leptons, which is controlled by the triplet vev v_t . The branching ratios of the doubly charged Higgs to muons for the benchmark v_t s are mentioned in Table 1.

While generating both the signal and the SM background events in `MadGraph5@NLO` [81], we employ the following pre-selection cuts used for ILC :

$$|\eta(\ell)| < 2.5; \quad p_T(\ell) > 10 \text{ GeV}; \quad \Delta R_{\ell\ell} \geq 0.4. \quad (4.1)$$

To generate the signal events for the muon collider, the following set of pre-selection cuts has been used:

$$|\eta(\ell)| < 3.0; \quad p_T(\ell) > 10 \text{ GeV}; \quad \Delta R_{\ell\ell} \geq 0.2. \quad (4.2)$$

The events are then passed to PYTHIA8[82] for hadronization, and finally detector simulation is performed using DELPHESv3[83] with the help of the appropriate muon collider card [84] for IMCC and the ILD card [85] for ILC.

\sqrt{s}	Cross-section	BP1	BP2	BP3	SM Background
500 GeV	$\sigma_{\text{ILC}}^{\text{DY}} \text{ (fb)}$	12.18	7.18	0.62	0.64
10 TeV	$\sigma_{\text{ILC}}^{\text{DY}} \text{ (fb)}$	1.12×10^{-6}	2.78×10^{-6}	3.16×10^{-6}	9.97×10^{-4}
500 GeV	$\sigma_{\text{IMCC}}^{\text{VBF}} \text{ (fb)}$	0.05	0.02	0.0001	-
10 TeV	$\sigma_{\text{IMCC}}^{\text{VBF}} \text{ (fb)}$	0.09	0.06	0.006	-

Table 2. Production cross-section of the signal processes in Drell-Yan as well as Vector Boson Fusion mode for our chosen benchmark points and the corresponding SM background at the ILC and muon collider for different center of mass energies.

4.1 Pair production of the doubly-charged Higgs via Drell-Yan process at the ILC

In this section, we discuss the prospects for detecting doubly charged LLPs produced in the Drell-Yan process at the 500 GeV ILC, followed by their decay to same-sign muon

pairs:

$$e^+e^- \rightarrow H^{++}H^{--}, H^{\pm\pm} \rightarrow \mu^\pm\mu^\pm. \quad (4.3)$$

The SM process that can mimic the signal comes from the di-boson background. We have generated inclusively $e^+e^- \rightarrow \mu^+\mu^+\mu^-\mu^-$. In addition to the basic cuts described in Eq. 4.1, we employ the following set of cuts to enhance the signal over the background:

- C1-1: We demand that the signal has exactly 4 muons and reject any other leptons, photons, and jets.
- C1-2: In Fig. 1, we plot the normalized distribution of the transverse momentum of the leading and sub-leading muons. For the signal, muons come from $H^{\pm\pm}$ and thus tend to peak in a slightly higher p_T bin, since the doubly-charged scalar mass is not that heavy. In the background, the leptons come from the gauge bosons. We put a moderate cut on the muon $p_T(\ell) > 30$ GeV.
- C1-3: We present the pseudorapidity distribution for both the signal and the background in Fig. 2. Since for the signal, the leptons are produced centrally, we put a cut of $|\eta_\ell| < 2.0$ to reduce the background.
- C1-4: In the context of LHC to search for a displaced vertex, an important variable impact parameter d_0 , is used in the literature to remove SM backgrounds [86–88]. Now, a track of a doubly charged scalar can be a very interesting signature for this kind of signal [15]. However, the reconstruction of that track in such an environment and the corresponding analysis is beyond the scope of our analysis and can be explored in the near future. The resolution of the vertices in the pixel tracker for both ATLAS and CMS detectors is of the order of hundreds μm [89, 90] and usually a cut of a few mm is imposed to suppress the SM background [50]. Compared to LHC, the sensitivity of the ILC pixel is of the order of a few μm [64], and one can expect that a little bit of displacement from the primary interaction point will be detected more efficiently at the ILC. In Fig. 3, we show the normalized distribution of the impact parameter d_0 of the leading and sub-leading muons. Since the muons are appearing from the long-lived $H^{\pm\pm}$, they are displaced from the primary vertex, and as a result, the daughter muons are also displaced. The transverse impact parameter d_0 exhibits an approximate dependence $\frac{1}{p_T}$ arising from the curvature of the track in the magnetic field [91]; consequently, benchmarks with higher muons p_T lead to smaller transverse impact parameters, as illustrated in Fig. 3. In the background, muons come from the W^\pm, Z prompt boson and are produced at the primary vertex. Finally, we

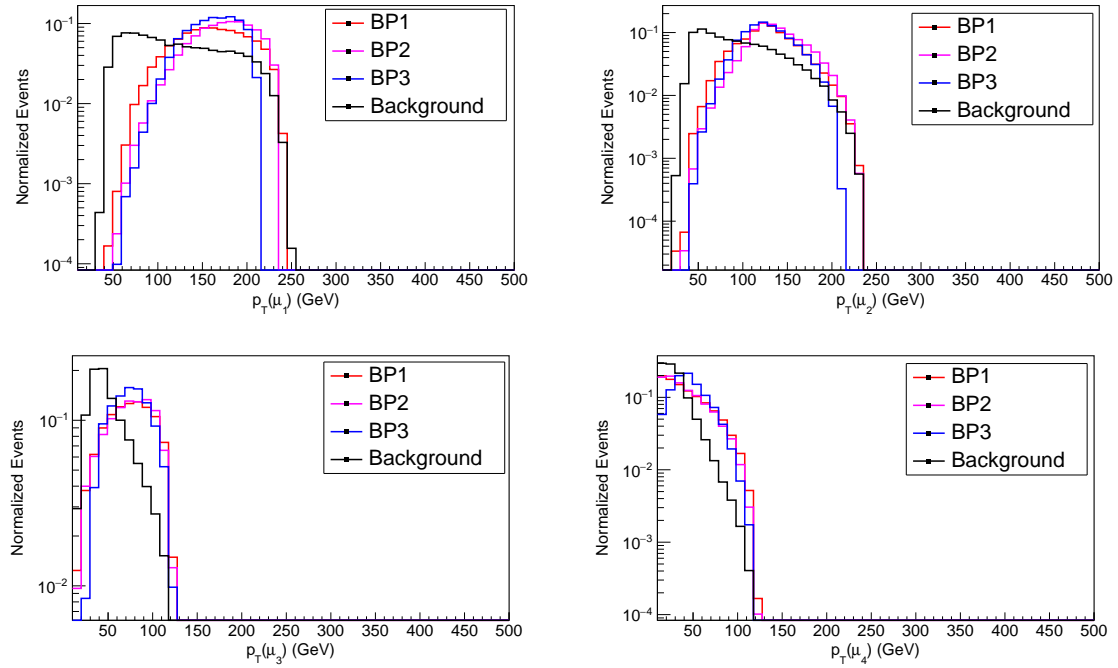


Figure 1. Normalized transverse momentum distributions of the leading and sub-leading muons in signal events are shown for benchmark points BP1, BP2, and BP3. For comparison, the corresponding Standard Model background distributions are also included. Results are presented for the ILC at $\sqrt{s} = 500$ GeV with integrated luminosity, $\mathcal{L}_{\text{int}} = 4\text{ab}^{-1}$.

demand 4 displaced muon tracks with $|d_0| > 0.01, 0.1(1)$ mm to remove the SM background completely. Here we would like to emphasize that even the signal muon with the smallest d_0 is demanded to be greater than > 0.1 mm.

Based on the cut-flow mentioned above, we quote the number of events at 4 ab^{-1} luminosity at the ILC in Table 3. The reach of the five signal events corresponds to an integrated luminosity of $\sim 3\text{ fb}^{-1}$ for BP1 and BP2, increasing to $\mathcal{O}(10^3)\text{ fb}^{-1}$ for BP3, as shown in Table 4.

Now, ILC can also be used as a discovery machine for the doubly-charged Higgs. In Fig. 4, we show the invariant mass distribution of the dimuons of the same-sign $M_{\mu^\pm\mu^\pm}$ after killing the SM background and see that for our chosen benchmark points, the invariant mass peaks at the exact bin with very little spread.

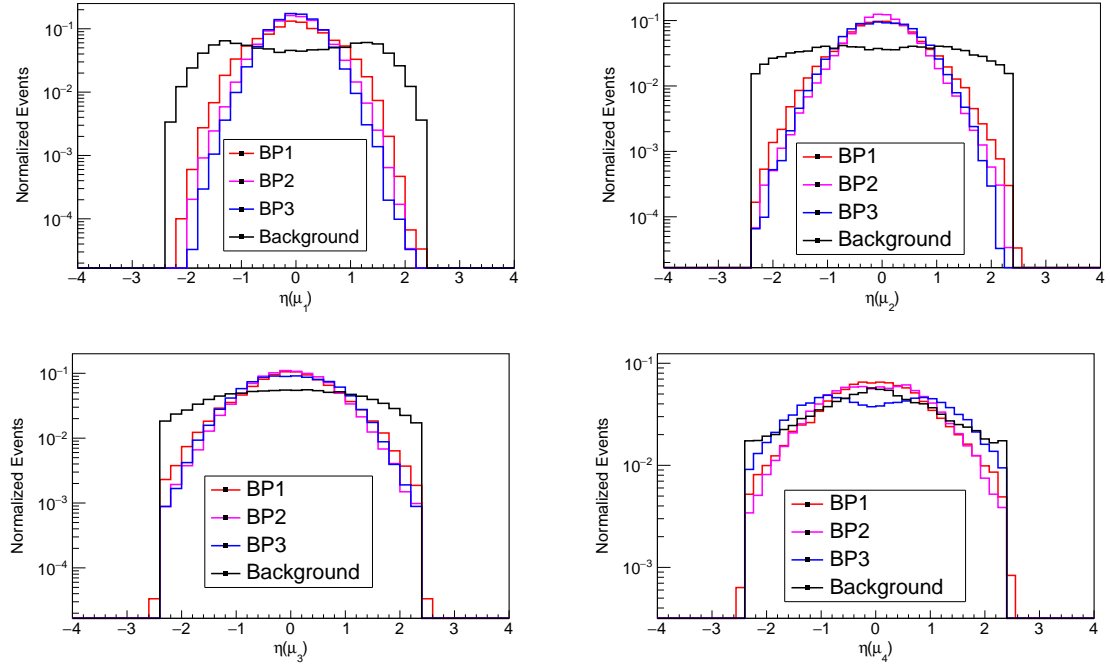


Figure 2. Normalized pseudo-rapidity distributions of the leading and sub-leading muons in signal events are shown for benchmark points BP1, BP2, and BP3. For comparison, the corresponding Standard Model background distributions are also included. Results are presented for the ILC at $\sqrt{s} = 500$ GeV with an integrated luminosity, $\mathcal{L}_{\text{int}} = 4ab^{-1}$.

Benchmark points	C1-1	C1-2	C1-3	C1-4		
				$d_0 > 0.01$ mm	$d_0 > 0.1$ mm	$d_0 > 1$ mm
BP1	29184	9021	18042	17662	16984	13278
BP2	16962	10286	10196	7270	7014	3628
BP3	1512	1222	1198	612	18	0
SM Background	1638	670	552	0	0	0

Table 3. Cut flow table showing the number of signal events at the ILC at $\mathcal{L}_{\text{int}} = 4ab^{-1}$ and $\sqrt{s} = 500$ GeV. The last three sub-columns show the final signal events after three choices of d_0 cut.

4.2 Pair production of doubly charged Higgs at muon collider with missing energy

For the pair production of doubly charged Higgs, when the minimal signal is just the Higgs pair, the next-to-minimal signal appears to be a pair of charged Higgs with a pair of fermions. We find that the inclusive production cross-section of a doubly charged Higgs with a pair of neutrinos is ~ 3 times larger than the production cross-section of

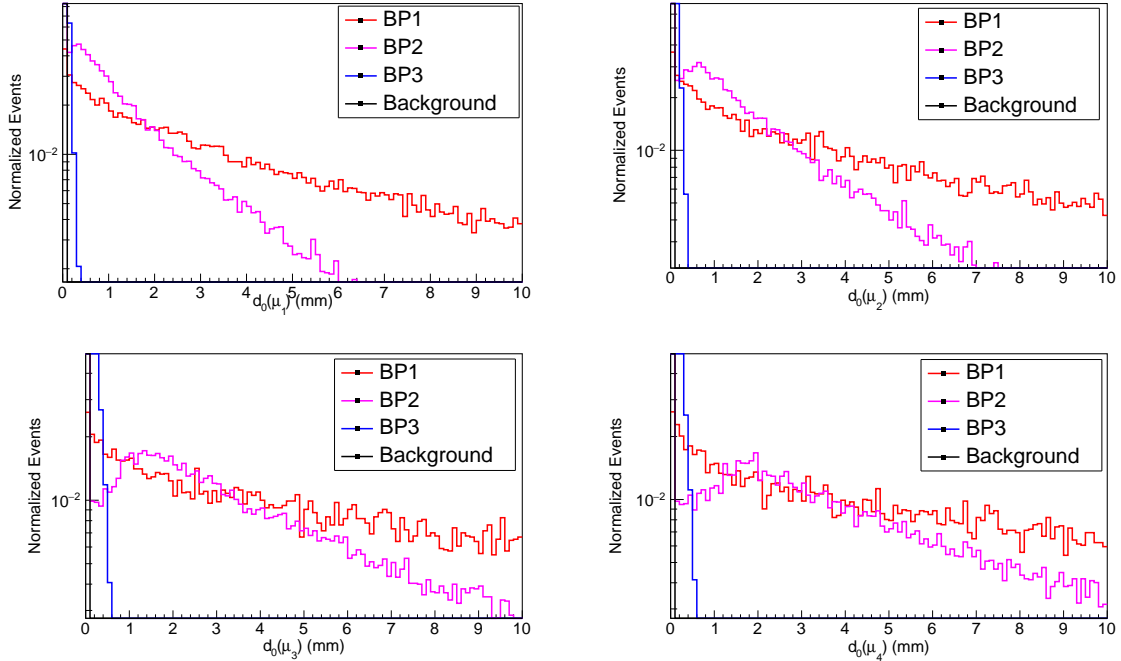


Figure 3. Normalized impact parameter $|d_0|$ distributions of the leading and sub-leading muons in signal events as well as the SM background. Results are presented for the ILC at $\sqrt{s} = 500$ GeV with an integrated luminosity, $\mathcal{L}_{\text{int}} = 4\text{ab}^{-1}$.

Benchmark Points	Luminosity required for 5 events after $ d_0 > 0.1\text{mm}$ cut (\mathcal{L}_5) (fb^{-1})
BP1	1.1
BP2	2.9
BP3	1111.1

Table 4. Luminosity required to see 5 signal events at the ILC.

only a pair of doubly charged Higgs at a 10 TeV muon collider. Therefore, we stick to the signal of four muons with missing energy at the muon collider. As a lepton collider has been considered here, the fermions must be a pair of charged or neutral leptons. The generation of the signal process is mentioned below:

$$\mu^+ \mu^- \rightarrow H^{++} H^{--} x \ y, H^{\pm\pm} \rightarrow \mu^\pm \mu^\pm$$

where $\{x = \mu^\pm, \nu_\ell\}$, $\{y = \mu^\mp, \nu_\ell\}$.

Although the dominant contribution to the signal should have come from the vector boson fusion (W^+W^-) and photon fusion, we found that the total cross-section

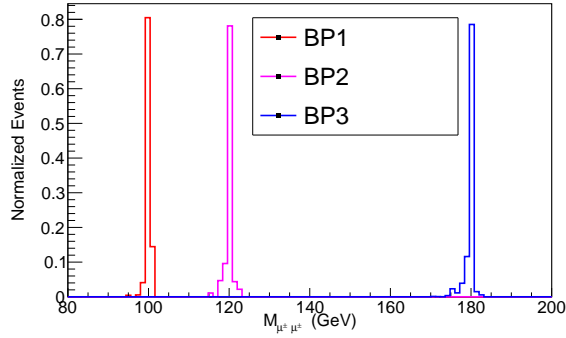


Figure 4. Normalized invariant mass distribution for same-sign dimuon pair for 3 chosen benchmark points at the ILC with an integrated luminosity, $\mathcal{L}_{\text{int}} = 4 \text{ab}^{-1}$.

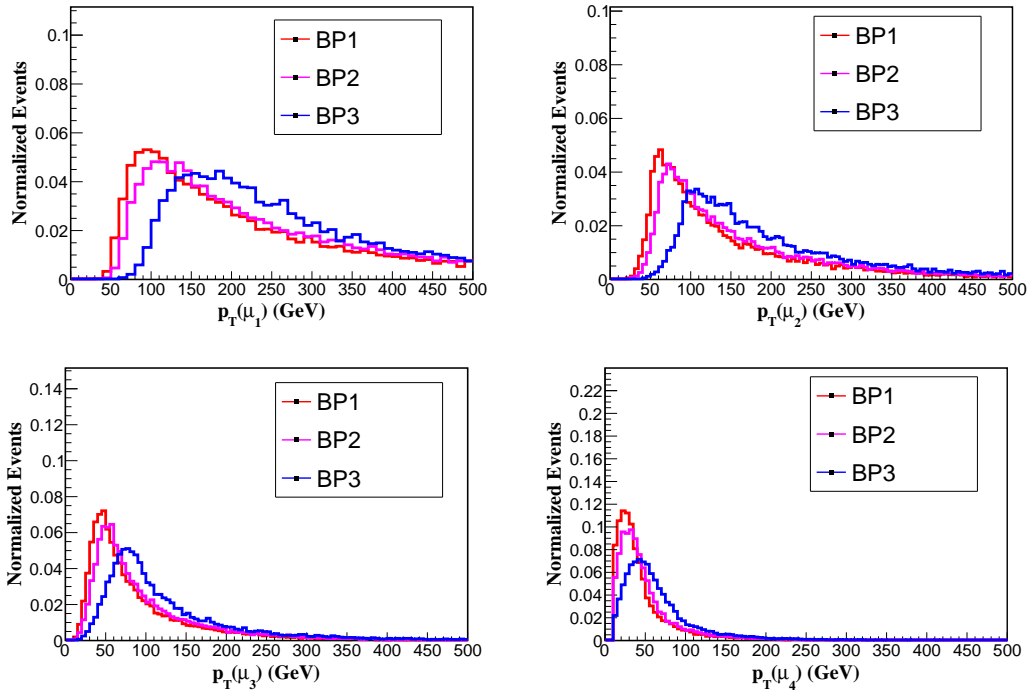


Figure 5. Normalized transverse momentum distributions of the leading and sub-leading muons in signal events are shown for benchmark points BP1, BP2, and BP3. Results are presented for the muon collider at $\sqrt{s} = 10 \text{ TeV}$ with $\mathcal{L}_{\text{int}} = 10 \text{ ab}^{-1}$.

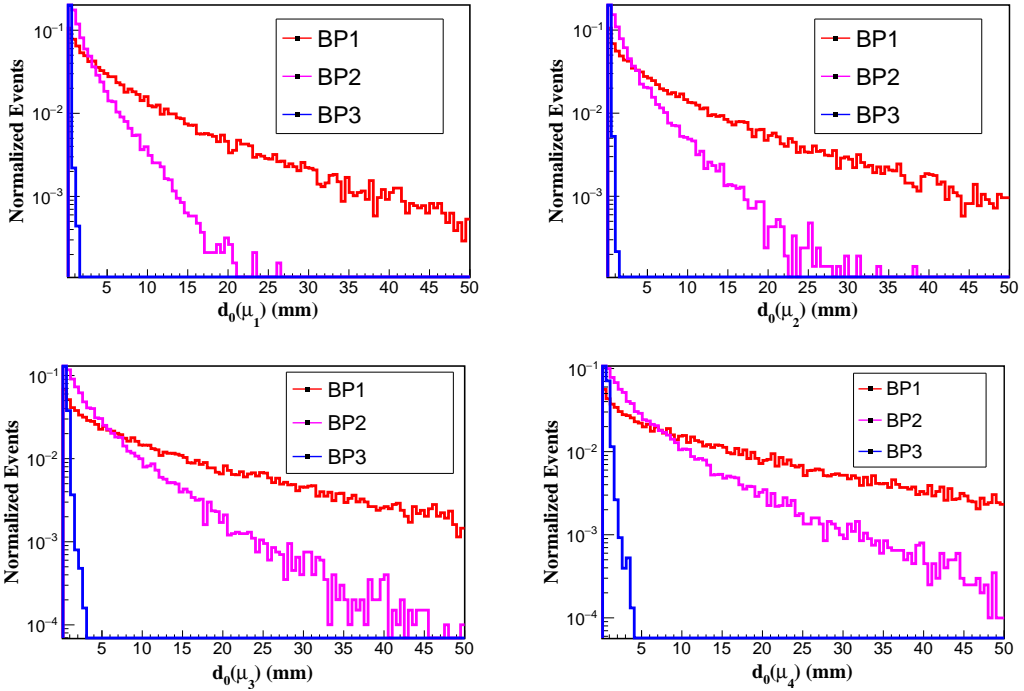


Figure 6. Normalized distribution of the $|d_0|$ variable of the leading and sub-leading muons for signal benchmark points BP1, BP2, and BP3 at muon collider with $\sqrt{s} = 10$ TeV with $\mathcal{L}_{\text{int}} = 10 \text{ ab}^{-1}$.

is significantly less than the individual contribution of the vector boson fusion processes. Due to the presence of a very large number of possible diagrams (involving new physics particles), we have considered an inclusive generation of the signal. Due to the very high CM energy, the two neutrinos or the two muons emitted from the primary vertex would be very close to the beam axis, consequently out of reach for the designed detectors. Therefore, not only the neutrinos, but also the muons along the beamline, would contribute to the missing energy in this process. The following SM processes can mimic our signal: triple vector boson processes (ZZZ , ZW^+W^- , γ (offshell) W^+W^- , γ (offshell) ZZ , γ (offshell) γ (offshell) Z). For a four-lepton final state with missing energy, the number of events coming from these processes is negligible due to the small leptonic branching ratios of the W^\pm and Z bosons and the additional suppression arising from $\alpha_{em} \approx \mathcal{O}(10^{-2})$. These background events are so tiny that they have hardly any impact on the d_0 distributions. Hence, we only present the signal distribution of the variable d_0 for our benchmark points based on cut-based analysis.

1. C2-1: In the first step, we select events with exactly four p_T ordered muons.

2. C2-2: In the next stage, sequential p_T cuts have been used on muons and events with $p_T(\ell_1) > 30$ GeV, $p_T(\ell_2) > 25$ GeV, $p_T(\ell_3) > 25$ GeV, $p_T(\ell_4) > 20$ GeV have been selected. The corresponding p_T distribution of the muons before applying any cut is presented in Fig. 5.
3. C2-3: The angular coverage of the upcoming muon collider goes from 10° to 170° [63], which corresponds to pseudo-rapidity in the range $-2.46 < \eta < 2.46$. We conservatively select the four muon events with $|\eta(\ell_i)| < 2.2$.
4. C2-4: Here, we demand a minimum of $\Delta R > 0.2$ cut on the same sign muons. To avoid fake missing transverse energy events due to the detector resolution effect, we impose a hard cut on missing transverse energy $\cancel{E}_T > 30.0$ GeV.
5. C2-5: Finally, to investigate the long-livedness of the doubly charged scalar, we put a cut over the d_0 variable of the muons while selecting the events. As shown in Fig. 6, the $|d_0|$ distribution of the benchmark 3 peaks is mainly around the zero value, which is also consistent with the decay length for that particular value of the doubly charged mass. According to the recent proposal of the muon collider detector design [63], as $d_0 < 0.1$ mm is taken for prompt decays, $d_0 > 0.1$ mm can be considered as a signature of long-lived decays. Therefore, the cuts used on the variable d_0 of the four muons are, respectively, $|d_0| > 0.1, 1$ mm. The $|d_0|$ distributions of the muons are shown in Fig. 6.

The corresponding SM backgrounds for this process are already very small; as a result, no background events survive after applying the above set of cuts in our simulation. In Tab. 5, we show the number of events that survive after giving all the aforementioned cuts at an integrated luminosity of 10ab^{-1} . The integrated luminosity required to see 5 signal events is $\sim 155(256)\text{fb}^{-1}$ for BP1(BP2), as mentioned in Tab. 6. These results show that a high-energy muon collider can also act as a discovery machine for doubly charged scalars, comparable to the ILC in the mass range (100-150) GeV. In Fig. 7, we show the invariant mass distribution of same-sign dimuons for two benchmark points after applying all the mentioned cuts, providing a distinct way for the discovery of a doubly charged scalar.

Here, we comment on the beam-induced background (BIB) [92, 93], which is a major issue in the muon collider environment. The initial muons decay on their way to flight, producing fluxes of electrons, photons, and neutrinos that create a large background near the beamline. However, here, restricting ourselves to the central region of the detector ($|\eta| < 2.2$) and demanding events with only muons, we avoid these background contaminations.

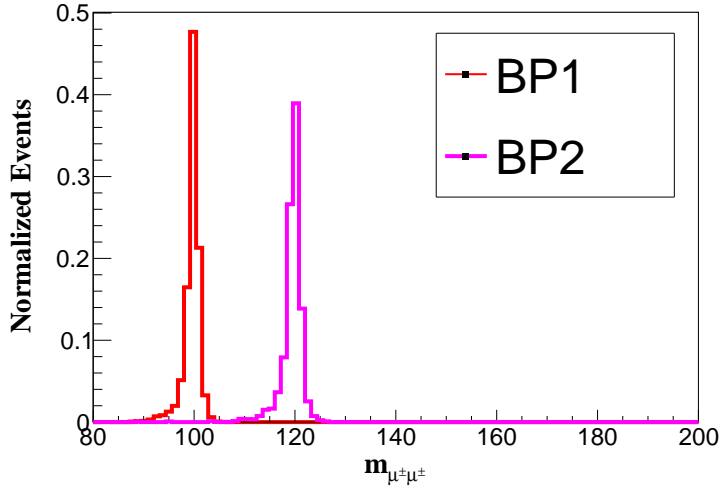


Figure 7. Normalized distribution of invariant mass of the same-sign di-muons for BP1 and BP2 at muon collider at $\sqrt{s} = 10$ TeV with $\mathcal{L}_{\text{int}} = 10 \text{ ab}^{-1}$.

Benchmark points	C2-1	C2-2	C2-3	C2-4	C2-5	
					$d_0 > 0.1 \text{ mm}$	$d_0 > 1 \text{ mm}$
BP1	512	406	353	343	323	234
BP2	338	289	247	239	195	66
BP3	36	33	28	27	<1	<1

Table 5. Cut flow table showing the number of signal events at the muon collider at $\mathcal{L}_{\text{int}} = 10 \text{ ab}^{-1}$ and $\sqrt{s} = 10$ TeV. The last two columns show the final signal events after two choices of d_0 cut.

Benchmark Points	\mathcal{L}_{int} required to see 5 events after $ d_0 > 0.1 \text{ mm}$ cut (fb^{-1})
BP1	155
BP2	256
BP3	-

Table 6. Integrated luminosity required to see 5 events at the muon collider with $\sqrt{s} = 10$ TeV. The symbol “-” for the BP3 benchmark point represents almost zero signal events after all cuts.

5 Conclusion

In this paper, we investigate the discovery prospects of long-lived doubly charged scalars at future lepton colliders within the framework of the Type-II seesaw model. Focusing on the parameter region where the doubly charged scalar behaves as a long-lived particle, we identified viable benchmark choices that satisfy all current theoretical and experimental constraints and are accessible at the ILC and a high-energy muon collider. We demonstrate that the search strategies at these facilities are chosen on the basis of the proposed CM of energy of the upcoming colliders. At ILC, with center-of-mass energies of 500 GeV, pair production of doubly charged scalars via the Drell-Yan process provides a clean and efficient probe in the same-sign dimuon channel. At the muon collider operating at 10 TeV energies, the production of $H^{\pm\pm}$ through vector boson fusion becomes dominant, allowing searches in the $\mu^\pm\mu^\pm + \cancel{E}_T$ final state. In both cases, Standard Model backgrounds can be effectively suppressed by exploiting displaced vertex information through a cut on the impact parameter d_0 . Our analysis shows that long-lived doubly charged scalars with masses in the range [100–180] GeV can be probed at these future lepton colliders. We observe that an integrated luminosity of $\sim 3 \text{ fb}^{-1}$ is sufficient to obtain five signal events at the ILC, while $\sim 250 \text{ fb}^{-1}$ is required at the muon collider for BP1 and BP2. Since for the choice of benchmark point BP3, the doubly-charged scalar has a very low proper decay length, it cannot be probed at the muon collider and requires integrated luminosity $\mathcal{O}(1) \text{ ab}^{-1}$ at the ILC to see at least 5 events.

Furthermore, the clean experimental environment of lepton colliders enables efficient mass reconstruction from same-sign dimuon pairs, significantly enhancing the discovery potential. These results highlight the unique capability of future lepton colliders to explore long-lived particle signatures and provide a compelling physics case for their role in probing extended scalar sectors beyond the SM.

Acknowledgement

ND thanks Debajyoti Choudhury, Rameswar Sahu, Purnath Unnikrishnan, Yashasvi and Vineet Kumar Jha for useful physics discussions. ND thanks Amit Adhikary regarding numerical simulations. ND’s work is supported by ANRF CRG/2023/008234. NG’s work is supported by the Japan Society for the Promotion of Science (JSPS) as part of the JSPS Postdoctoral Program (Standard), grant number: JP24KF0189, and by the World Premier International Research Center Initiative (WPI), MEXT,

Japan (Kavli IPMU). NG and ND would also like to thank Indian Association for the Cultivation of Science(IACS) for hospitality where the part of the project was done.

References

- [1] **ATLAS** Collaboration, G. Aad et al., *Observation of a new particle in the search for the Standard Model Higgs boson with the ATLAS detector at the LHC*, *Phys. Lett. B* **716** (2012) 1–29, [[arXiv:1207.7214](https://arxiv.org/abs/1207.7214)].
- [2] **CMS** Collaboration, S. Chatrchyan et al., *Observation of a New Boson at a Mass of 125 GeV with the CMS Experiment at the LHC*, *Phys. Lett. B* **716** (2012) 30–61, [[arXiv:1207.7235](https://arxiv.org/abs/1207.7235)].
- [3] **Particle Data Group** Collaboration, S. Navas et al., *Review of particle physics*, *Phys. Rev. D* **110** (2024), no. 3 030001.
- [4] S. Knapen and S. Lowette, *A Guide to Hunting Long-Lived Particles at the LHC*, *Ann. Rev. Nucl. Part. Sci.* **73** (2023) 421–449, [[arXiv:2212.03883](https://arxiv.org/abs/2212.03883)].
- [5] T. Bose et al., *Report of the Topical Group on Physics Beyond the Standard Model at Energy Frontier for Snowmass 2021*, [arXiv:2209.13128](https://arxiv.org/abs/2209.13128).
- [6] **SHiP** Collaboration, K. Y. Lee, *New physics searches with SHiP*, *PoS NuFact2019* (2019) 107.
- [7] **NA62** Collaboration, G. Lanfranchi, *Search for Hidden Sector particles at NA62*, *PoS EPS-HEP2017* (2017) 301.
- [8] **NA64** Collaboration, D. Banerjee et al., *Search for Axionlike and Scalar Particles with the NA64 Experiment*, *Phys. Rev. Lett.* **125** (2020), no. 8 081801, [[arXiv:2005.02710](https://arxiv.org/abs/2005.02710)].
- [9] A. Belyaev, S. Moretti, K. Nickel, M. C. Thomas, and I. Tomalin, *Hunting for neutral, long-lived exotica at the LHC using a missing transverse energy signature*, *JHEP* **03** (2016) 018, [[arXiv:1512.02229](https://arxiv.org/abs/1512.02229)].
- [10] **FASER** Collaboration, A. Ariga et al., *FASER’s physics reach for long-lived particles*, *Phys. Rev. D* **99** (2019), no. 9 095011, [[arXiv:1811.12522](https://arxiv.org/abs/1811.12522)].
- [11] M. Cepeda, S. Gori, V. M. Outschoorn, and J. Shelton, *Exotic Higgs Decays*, [arXiv:2111.12751](https://arxiv.org/abs/2111.12751).
- [12] D. Curtin and J. S. Grewal, *Long Lived Particle Decays in MATHUSLA*, *Phys. Rev. D* **109** (2024), no. 7 075017, [[arXiv:2308.05860](https://arxiv.org/abs/2308.05860)].
- [13] E. Akhmedov, P. S. B. Dev, S. Jana, and R. N. Mohapatra, *Long-lived doubly charged scalars in the left-right symmetric model: Catalyzed nuclear fusion and collider implications*, *Phys. Lett. B* **852** (2024) 138616, [[arXiv:2401.15145](https://arxiv.org/abs/2401.15145)].

[14] **ATLAS** Collaboration, G. Aad et al., *ATLAS searches for additional scalars and exotic Higgs boson decays with the LHC Run 2 dataset*, *Phys. Rept.* **1116** (2025) 184–260, [[arXiv:2405.04914](https://arxiv.org/abs/2405.04914)].

[15] C.-T. Lu, X. Wang, X. Wei, and Y. Wu, *Probing long-lived doubly charged scalar in the Georgi-Machacek model at the LHC and in far detectors*, *JHEP* **02** (2025) 149, [[arXiv:2410.19561](https://arxiv.org/abs/2410.19561)].

[16] **ATLAS** Collaboration, G. Aad et al., *Search for displaced leptons in $\sqrt{s} = 13$ TeV and 13.6 TeV pp collisions with the ATLAS detector*, *Phys. Rev. D* **112** (2025), no. 1 012016, [[arXiv:2410.16835](https://arxiv.org/abs/2410.16835)].

[17] J. Alimena et al., *Feebly-Interacting Particles: FIPs at LHCb — Workshop Report 2025 Edition*, in *LHCb FIP Physics Workshop 2025*, 10, 2025. [arXiv:2510.05257](https://arxiv.org/abs/2510.05257).

[18] Y. Fang, W. Su, X. Wang, Y. Wu, and Y. Zhang, *Search for Light Neutral Scalar in the Georgi-Machacek Model with Forward Detectors at the LHC*, [arXiv:2512.19151](https://arxiv.org/abs/2512.19151).

[19] **ILD** Collaboration, J. Klamka and A. F. Zarnecki, *Searching for displaced vertices with a gaseous tracker for a future e^+e^- Higgs factory*, *JHEP* **02** (2025) 112, [[arXiv:2409.13492](https://arxiv.org/abs/2409.13492)].

[20] B. Bhattacherjee, S. Matsumoto, and R. Sengupta, *Long-lived light mediators from Higgs boson decay at HL-LHC and FCC-hh, and a proposal of dedicated long-lived particle detectors for FCC-hh*, *Phys. Rev. D* **106** (2022), no. 9 095018, [[arXiv:2111.02437](https://arxiv.org/abs/2111.02437)].

[21] B. Bhattacherjee, H. K. Dreiner, N. Ghosh, S. Matsumoto, R. Sengupta, and P. Solanki, *Light long-lived particles at the FCC-hh with the proposal for a dedicated forward detector FOREHUNT and a transverse detector DELIGHT*, *Phys. Rev. D* **110** (2024), no. 1 015036, [[arXiv:2306.11803](https://arxiv.org/abs/2306.11803)].

[22] B. Bhattacherjee, C. Bose, H. K. Dreiner, N. Ghosh, S. Matsumoto, and R. Sengupta, *Long-lived Light Mediators in a Higgs Portal Model at the FCC-ee*, [arXiv:2503.08780](https://arxiv.org/abs/2503.08780).

[23] B. Bhattacherjee, C. Bose, H. K. Dreiner, N. Ghosh, S. Matsumoto, S. Mukherjee, R. Sengupta, and A. Sharma, *Proposal for a shared transverse LLP detector for FCC-ee and FCC-hh and a forward LLP detector for FCC-hh*, [arXiv:2503.21875](https://arxiv.org/abs/2503.21875).

[24] B. Bhattacherjee, A. Kumar, S. Mukherjee, R. Sengupta, and A. Sharma, *From obstacle to opportunity: Uncovering the silver lining of pileup*, *Phys. Lett. B* **873** (2026) 140121, [[arXiv:2503.11760](https://arxiv.org/abs/2503.11760)].

[25] A. Filimonova, R. Schäfer, and S. Westhoff, *Probing dark sectors with long-lived particles at BELLE II*, *Phys. Rev. D* **101** (2020), no. 9 095006, [[arXiv:1911.03490](https://arxiv.org/abs/1911.03490)].

[26] P. S. B. Dev, B. Dutta, K. J. Kelly, R. N. Mohapatra, and Y. Zhang, *Light, long-lived*

*B – L gauge and Higgs bosons at the DUNE near detector, JHEP **07** (2021) 166, [[arXiv:2104.07681](https://arxiv.org/abs/2104.07681)].*

[27] B. Batell et al., *Dark Sector Studies with Neutrino Beams*, in *Snowmass 2021*, 7, 2022. [[arXiv:2207.06898](https://arxiv.org/abs/2207.06898)].

[28] J. Schechter and J. W. F. Valle, *Neutrino Masses in $SU(2) \times U(1)$ Theories, Phys. Rev. D* **22** (1980) 2227.

[29] M. Magg and C. Wetterich, *Neutrino Mass Problem and Gauge Hierarchy, Phys. Lett. B* **94** (1980) 61–64.

[30] T. P. Cheng and L.-F. Li, *Neutrino Masses, Mixings and Oscillations in $SU(2) \times U(1)$ Models of Electroweak Interactions, Phys. Rev. D* **22** (1980) 2860.

[31] G. Lazarides, Q. Shafi, and C. Wetterich, *Proton Lifetime and Fermion Masses in an $SO(10)$ Model, Nucl. Phys. B* **181** (1981) 287–300.

[32] R. N. Mohapatra and G. Senjanovic, *Neutrino Masses and Mixings in Gauge Models with Spontaneous Parity Violation, Phys. Rev. D* **23** (1981) 165.

[33] G. 't Hooft, *Naturalness, chiral symmetry, and spontaneous chiral symmetry breaking, NATO Sci. Ser. B* **59** (1980) 135–157.

[34] P. F. de Salas, D. V. Forero, C. A. Ternes, M. Tortola, and J. W. F. Valle, *Status of neutrino oscillations 2018: 3σ hint for normal mass ordering and improved CP sensitivity, Phys. Lett. B* **782** (2018) 633–640, [[arXiv:1708.01186](https://arxiv.org/abs/1708.01186)].

[35] P. Fileviez Perez, T. Han, G.-y. Huang, T. Li, and K. Wang, *Neutrino Masses and the CERN LHC: Testing Type II Seesaw, Phys. Rev. D* **78** (2008) 015018, [[arXiv:0805.3536](https://arxiv.org/abs/0805.3536)].

[36] A. Melfo, M. Nemevsek, F. Nesti, G. Senjanovic, and Y. Zhang, *Type II Seesaw at LHC: The Roadmap, Phys. Rev. D* **85** (2012) 055018, [[arXiv:1108.4416](https://arxiv.org/abs/1108.4416)].

[37] M. Aoki, S. Kanemura, and K. Yagyu, *Testing the Higgs triplet model with the mass difference at the LHC, Phys. Rev. D* **85** (2012) 055007, [[arXiv:1110.4625](https://arxiv.org/abs/1110.4625)].

[38] **ATLAS** Collaboration, M. Aaboud et al., *Search for doubly charged scalar bosons decaying into same-sign W boson pairs with the ATLAS detector, Eur. Phys. J. C* **79** (2019), no. 1 58, [[arXiv:1808.01899](https://arxiv.org/abs/1808.01899)].

[39] **ATLAS** Collaboration, G. Aad et al., *Search for doubly and singly charged Higgs bosons decaying into vector bosons in multi-lepton final states with the ATLAS detector using proton-proton collisions at $\sqrt{s} = 13$ TeV, JHEP **06** (2021) 146, [[arXiv:2101.11961](https://arxiv.org/abs/2101.11961)].*

[40] **ATLAS** Collaboration, G. Aad et al., *Search for doubly charged Higgs boson production*

*in multi-lepton final states using 139 fb^{-1} of proton–proton collisions at $\sqrt{s} = 13 \text{ TeV}$ with the ATLAS detector, *Eur. Phys. J. C* **83** (2023), no. 7 605, [[arXiv:2211.07505](#)].*

- [41] **ATLAS** Collaboration, *Search for doubly charged Higgs boson production in multi-lepton final states using 139 fb^{-1} of proton–proton collisions at $\sqrt{s} = 13 \text{ TeV}$ with the ATLAS detector, .*
- [42] **CMS** Collaboration, *A search for doubly-charged Higgs boson production in three and four lepton final states at $\sqrt{s} = 13 \text{ TeV}$, .*
- [43] **CMS** Collaboration, A. M. Sirunyan et al., *Observation of electroweak production of same-sign W boson pairs in the two jet and two same-sign lepton final state in proton–proton collisions at $\sqrt{s} = 13 \text{ TeV}$, *Phys. Rev. Lett.* **120** (2018), no. 8 081801, [[arXiv:1709.05822](#)].*
- [44] **CMS** Collaboration, A. M. Sirunyan et al., *Search for charged Higgs bosons produced in vector boson fusion processes and decaying into vector boson pairs in proton–proton collisions at $\sqrt{s} = 13 \text{ TeV}$, *Eur. Phys. J. C* **81** (2021), no. 8 723, [[arXiv:2104.04762](#)].*
- [45] **ATLAS** Collaboration, *Search for heavy long-lived multi-charged particles in the full Run-II pp collision data at $\sqrt{s} = 13 \text{ TeV}$ using the ATLAS detector, .*
- [46] **ATLAS** Collaboration, G. Aad et al., *Search for heavy long-lived multi-charged particles in the full LHC Run 2 pp collision data at $s=13 \text{ TeV}$ using the ATLAS detector, *Phys. Lett. B* **847** (2023) 138316, [[arXiv:2303.13613](#)].*
- [47] **CMS** Collaboration, V. Khachatryan et al., *Search for long-lived charged particles in proton–proton collisions at $\sqrt{s} = 13 \text{ TeV}$, *Phys. Rev. D* **94** (2016), no. 11 112004, [[arXiv:1609.08382](#)].*
- [48] **CMS** Collaboration, *Search for heavy long-lived charged particles with Level-1 Scouting data from proton–proton collisions at $\sqrt{s} = 13.6 \text{ TeV}$, .*
- [49] P. S. Bhupal Dev and Y. Zhang, *Displaced vertex signatures of doubly charged scalars in the type-II seesaw and its left-right extensions*, *JHEP* **10** (2018) 199, [[arXiv:1808.00943](#)].
- [50] S. Antusch, O. Fischer, A. Hammad, and C. Scherb, *Low scale type II seesaw: Present constraints and prospects for displaced vertex searches*, *JHEP* **02** (2019) 157, [[arXiv:1811.03476](#)].
- [51] **ILC** Collaboration, G. Aarons et al., *ILC Reference Design Report Volume 1 - Executive Summary*, [arXiv:0712.1950](#).
- [52] **ILC** Collaboration, G. Aarons et al., *International Linear Collider Reference Design Report Volume 2: Physics at the ILC*, [arXiv:0709.1893](#).
- [53] **ILC** Collaboration, G. Aarons et al., *ILC Reference Design Report Volume 4 - Detectors*, [arXiv:0712.2356](#).

[54] **ILC** Collaboration, *The International Linear Collider Progress Report 2015*, .

[55] **ILC** Collaboration, H. Aihara et al., *The International Linear Collider. A Global Project*, [arXiv:1901.09829](https://arxiv.org/abs/1901.09829).

[56] Y. Abe et al., *Status of the International Linear Collider*, [arXiv:2505.11292](https://arxiv.org/abs/2505.11292).

[57] “International Muon Collider Collaboration.” <https://muoncollider.web.cern.ch/>.

[58] J. P. Delahaye, M. Diemoz, K. Long, B. Mansoulié, N. Pastrone, L. Rivkin, D. Schulte, A. Skrinsky, and A. Wulzer, *Muon Colliders*, [arXiv:1901.06150](https://arxiv.org/abs/1901.06150).

[59] D. Schulte, J.-P. Delahaye, M. Diemoz, K. Long, B. Mansoulié, N. Patrone, L. Rivkin, A. M. Skrinsky, and A. Wulzer, *Muon Collider. A Path to the Future?*, *PoS EPS-HEP2019* (2020) 004.

[60] **International Muon Collider** Collaboration, D. Schulte, *The Muon Collider*, *JACoW IPAC2022* (2022) 821–826.

[61] **International Muon Collider** Collaboration, C. Accettura et al., *Interim report for the International Muon Collider Collaboration (IMCC)*, *CERN Yellow Rep. Monogr. 2/2024* (2024) 176, [[arXiv:2407.12450](https://arxiv.org/abs/2407.12450)].

[62] M. Begel et al., *United States Muon Collider Community White Paper for the European Strategy for Particle Physics Update*, [arXiv:2503.23695](https://arxiv.org/abs/2503.23695).

[63] **International Muon Collider** Collaboration, C. Accettura et al., *The Muon Collider*, [arXiv:2504.21417](https://arxiv.org/abs/2504.21417).

[64] **ILC International Development Team** Collaboration, A. Aryshev et al., *The International Linear Collider: Report to Snowmass 2021*, [arXiv:2203.07622](https://arxiv.org/abs/2203.07622).

[65] A. Costantini, F. De Lillo, F. Maltoni, L. Mantani, O. Mattelaer, R. Ruiz, and X. Zhao, *Vector boson fusion at multi-TeV muon colliders*, *JHEP* **09** (2020) 080, [[arXiv:2005.10289](https://arxiv.org/abs/2005.10289)].

[66] T. Han, Y. Ma, and K. Xie, *High energy leptonic collisions and electroweak parton distribution functions*, *Phys. Rev. D* **103** (2021), no. 3 L031301, [[arXiv:2007.14300](https://arxiv.org/abs/2007.14300)].

[67] A. Arhrib, R. Benbrik, M. Chabab, G. Moultaka, M. C. Peyranere, L. Rahili, and J. Ramadan, *The Higgs Potential in the Type II Seesaw Model*, *Phys. Rev. D* **84** (2011) 095005, [[arXiv:1105.1925](https://arxiv.org/abs/1105.1925)].

[68] D. K. Ghosh, N. Ghosh, I. Saha, and A. Shaw, *Revisiting the high-scale validity of the type II seesaw model with novel LHC signature*, *Phys. Rev. D* **97** (2018), no. 11 115022, [[arXiv:1711.06062](https://arxiv.org/abs/1711.06062)].

[69] P. S. Bhupal Dev, D. K. Ghosh, N. Okada, and I. Saha, *125 GeV Higgs Boson and the Type-II Seesaw Model*, *JHEP* **03** (2013) 150, [[arXiv:1301.3453](https://arxiv.org/abs/1301.3453)]. [Erratum: *JHEP* 05, 049 (2013)].

[70] C. Bonilla, J. C. Romão, and J. W. F. Valle, *Electroweak breaking and neutrino mass: ‘invisible’ Higgs decays at the LHC (type II seesaw)*, *New J. Phys.* **18** (2016), no. 3 033033, [[arXiv:1511.07351](https://arxiv.org/abs/1511.07351)].

[71] L. Lavoura and L.-F. Li, *Making the small oblique parameters large*, *Phys. Rev. D* **49** (1994) 1409–1416, [[hep-ph/9309262](https://arxiv.org/abs/hep-ph/9309262)].

[72] M. Aoki, S. Kanemura, M. Kikuchi, and K. Yagyu, *Radiative corrections to the Higgs boson couplings in the triplet model*, *Phys. Rev. D* **87** (2013), no. 1 015012, [[arXiv:1211.6029](https://arxiv.org/abs/1211.6029)].

[73] E. J. Chun, H. M. Lee, and P. Sharma, *Vacuum Stability, Perturbativity, EWPD and Higgs-to-diphoton rate in Type II Seesaw Models*, *JHEP* **11** (2012) 106, [[arXiv:1209.1303](https://arxiv.org/abs/1209.1303)].

[74] CMS Collaboration, A. Tumasyan et al., *A portrait of the Higgs boson by the CMS experiment ten years after the discovery.*, *Nature* **607** (2022), no. 7917 60–68, [[arXiv:2207.00043](https://arxiv.org/abs/2207.00043)]. [Erratum: *Nature* 623, (2023)].

[75] ALEPH, DELPHI, L3, OPAL, LEP Collaboration, G. Abbiendi et al., *Search for Charged Higgs bosons: Combined Results Using LEP Data*, *Eur. Phys. J. C* **73** (2013) 2463, [[arXiv:1301.6065](https://arxiv.org/abs/1301.6065)].

[76] ATLAS Collaboration, G. Aad et al., *Search for charged Higgs bosons produced in top-quark decays or in association with top quarks and decaying via $H^\pm \rightarrow \tau^\pm \nu \tau$ in 13 TeV pp collisions with the ATLAS detector*, *Phys. Rev. D* **111** (2025), no. 7 072006, [[arXiv:2412.17584](https://arxiv.org/abs/2412.17584)].

[77] ATLAS Collaboration, G. Aad et al., *Search for a heavy charged Higgs boson decaying into a W boson and a Higgs boson in final states with leptons and b-jets in $\sqrt{s} = 13$ TeV pp collisions with the ATLAS detector*, *JHEP* **02** (2025) 143, [[arXiv:2411.03969](https://arxiv.org/abs/2411.03969)].

[78] ATLAS Collaboration, M. Aaboud et al., *Search for heavy resonances decaying into WW in the $e\nu\mu\nu$ final state in pp collisions at $\sqrt{s} = 13$ TeV with the ATLAS detector*, *Eur. Phys. J. C* **78** (2018), no. 1 24, [[arXiv:1710.01123](https://arxiv.org/abs/1710.01123)].

[79] ATLAS Collaboration, G. Aad et al., *Search for heavy resonances decaying into a pair of Z bosons in the $\ell^+\ell^-\ell'^+\ell'^-$ and $\ell^+\ell^-\nu\bar{\nu}$ final states using 139 fb^{-1} of proton–proton collisions at $\sqrt{s} = 13$ TeV with the ATLAS detector*, *Eur. Phys. J. C* **81** (2021), no. 4 332, [[arXiv:2009.14791](https://arxiv.org/abs/2009.14791)].

[80] Z. Kang, J. Li, T. Li, Y. Liu, and G.-Z. Ning, *Light Doubly Charged Higgs Boson via the WW* Channel at LHC*, *Eur. Phys. J. C* **75** (2015), no. 12 574, [[arXiv:1404.5207](https://arxiv.org/abs/1404.5207)].

[81] J. Alwall, R. Frederix, S. Frixione, V. Hirschi, F. Maltoni, O. Mattelaer, H. S. Shao, T. Stelzer, P. Torrielli, and M. Zaro, *The automated computation of tree-level and*

*next-to-leading order differential cross sections, and their matching to parton shower simulations, JHEP **07** (2014) 079, [[arXiv:1405.0301](https://arxiv.org/abs/1405.0301)].*

- [82] T. Sjöstrand, S. Ask, J. R. Christiansen, R. Corke, N. Desai, P. Ilten, S. Mrenna, S. Prestel, C. O. Rasmussen, and P. Z. Skands, *An introduction to PYTHIA 8.2*, *Comput. Phys. Commun.* **191** (2015) 159–177, [[arXiv:1410.3012](https://arxiv.org/abs/1410.3012)].
- [83] **DELPHES 3** Collaboration, J. de Favereau, C. Delaere, P. Demin, A. Giannanco, V. Lemaître, A. Mertens, and M. Selvaggi, *DELPHES 3, A modular framework for fast simulation of a generic collider experiment*, *JHEP* **02** (2014) 057, [[arXiv:1307.6346](https://arxiv.org/abs/1307.6346)].
- [84] C. Collaboration, “Delphes card for muon collider.”
https://indico.cern.ch/event/957299/contributions/4023467/attachments/2106044/3541874/delphes_card_muocol_mdi_.pdf, 2020.
- [85] H. Abramowicz et al., *The International Linear Collider Technical Design Report - Volume 4: Detectors*, [arXiv:1306.6329](https://arxiv.org/abs/1306.6329).
- [86] **ATLAS** Collaboration, G. Aad et al., *Search for long-lived, heavy particles in final states with a muon and multi-track displaced vertex in proton-proton collisions at $\sqrt{s} = 7$ TeV with the ATLAS detector*, *Phys. Lett. B* **719** (2013) 280–298, [[arXiv:1210.7451](https://arxiv.org/abs/1210.7451)].
- [87] D. G. Cerdeño, V. Martín-Lozano, and O. Seto, *Displaced vertices and long-lived charged particles in the NMSSM with right-handed sneutrinos*, *JHEP* **05** (2014) 035, [[arXiv:1311.7260](https://arxiv.org/abs/1311.7260)].
- [88] W. Abdallah, A. Hammad, A. Kasem, and S. Khalil, *Long-lived B-L symmetric SSM particles at the LHC*, *Phys. Rev. D* **98** (2018), no. 9 095019, [[arXiv:1804.09778](https://arxiv.org/abs/1804.09778)].
- [89] **ATLAS** Collaboration, D. Kobayashi, *Module development for the Phase-2 ATLAS ITk Pixel upgrade*, *JINST* **14** (2019), no. 09 C09036.
- [90] **CMS Tracker Group** Collaboration, W. Adam et al., *Evaluation of 3D pixel silicon sensors for the CMS Phase-2 Inner Tracker*, [arXiv:2510.13304](https://arxiv.org/abs/2510.13304).
- [91] T. Han, *Collider phenomenology: Basic knowledge and techniques*, in *Theoretical Advanced Study Institute in Elementary Particle Physics: Physics in $D \geq 4$* , pp. 407–454, 8, 2005. [hep-ph/0508097](https://arxiv.org/abs/hep-ph/0508097).
- [92] N. Bartosik, A. Bertolin, L. Buonincontri, M. Casarsa, F. Collamati, A. Ferrari, A. Ferrari, A. Gianelle, D. Lucchesi, N. Mokhov, M. Palmer, N. Pastrone, P. Sala, L. Sestini, and S. Striganov, *Detector and physics performance at a muon collider*, *Journal of Instrumentation* **15** (may, 2020) P05001.
- [93] N. Mokhov and S. Striganov, *Detector backgrounds at muon colliders*, *Physics Procedia* **37** (2012) 2015–2022. Proceedings of the 2nd International Conference on Technology and Instrumentation in Particle Physics (TIPP 2011).